Egyptian Journal of Pure and Applied Science

Use of 3D Post-stack Seismic Inversion for Quantitative Subsurface Interpretation at Simian Gas Field, Egypt's Offshore West Nile Delta

Abdel Nasser M. A. Helal[1], Karam S. I. Farag[1] and Ahmed Hosny[2*]

[1] *Geophysics Department, Faculty of Science, Ain Shams University, Abbassia 11566, Cairo, Egypt,*
[2] *Rashid Petroleum Company (RASHPETCO), 18 Road 294, New Maadi, Cairo, Egypt*

ARTICLE INFO

Article history:
Received 12 June 2014
Accepted 22 June 2014

Keywords:
Seismic inversion;
seismic reflection;
acoustic impedance;
Simian gas field;
west Nile Delta.

ABSTRACT

Seismic inversion is the procedure for extracting the multi-dimensional earth model of quantitative physical properties of a reservoir by combining both seismic reflection and well logging/core data. In most cases, the target physical parameters are the earth's acoustic impedance, seismic velocity and bulk density. Seismic attributes based on such an inversion are also utilized to improve the subsurface interpretation. The inversion procedure starts usually with mathematically-generated forward calculations of the earth's seismic response using a set of initial model parameters. The scope of this study is to undertake three-dimensional (3D) smoothed-earth post-stack seismic inversion trials for imaging both the subsurface lithological–structural fashion and fluid coverage within the Simian gas field at the Egypt's offshore west Nile Delta.

Introduction

In quantitative data interpretation flow, seismic inversion involves estimation of physical properties of the concerning earth model using seismic reflection data which are usually constrained by well logging/core data. With certain limitations, it can also be undertaken in areas where such solid data are exceptionally absent. Seismic inversion can be pre- or post-stack, deterministic, stochastic or geo-statistical. Selection of a specific inversion technique depends mainly on the subsurface characteristics. All techniques require estimated seismic wavelets from the reflection data. Typically, a reflection coefficient series from a stratigraphic-control well, with available sonic and density logs, located within the seismic survey coverage, is used to estimate the statistical wavelet phase and frequency. Accurate wavelet estimation requires the accurate tie of the impedance log to seismic data. Errors in well tie can result in phase and/or frequency artifacts in the estimation wavelet. Once the wavelet is identified, the most common action is to remove the wavelet tuning and interference effects which lead to the high-resolution display of the acoustic impedance volume, i.e. the product of primary seismic velocity times bulk density. The inversion results are then convolved with the earth's wavelet to produce synthetic (calculated) seismic traces which are iteratively compared (and updated) to the original (measured) traces [1].

* Corresponding author.
E-mail address: Ahmed.Hosny@RASHPETCO.com

General Geological Setting

Simian gas field is located in the eastern part of the West Delta Deep Marine (WDDM) concession, offshore Nile Delta, approximately 120 km northeast of Alexandria (northern Egypt) in water depths, ranging between 500 and 1,500 m (**Figure 1**). The field covers an area of some 200 km² and comprises major Pliocene turbidity complexes, consisting of varying reservoir quality sandstones/sands of a deep-water marine nature. Sandstones were deposited in a broadly north/northeast–south/southwest trending slope–channel system, draped on the western Nile Delta slope margin and pinched-out within the sealing El-Wastani Formation (sandy claystones) [2]. Since the field lies on the hanging-wall of the main Rosetta Fault, its architectural style and trapping mechanism are regionally thought to be formed via a combined stratigraphic–structural control [3,4].

Conventional Data Interpretation

The whole field was surveyed during 2006, and its high-quality three-dimensional (3D) seismic cube was later processed in 2007. No multiple reflections, or even small multiplicative events, were seen on stacked–migrated seismic sections, particularly in the vicinity of the target reservoir zone.

Data were extensively visualized, colored-contoured and conventionally interpreted using the integrated GeoFrame Reservoir Characterization Software (Schlumberger Limited, USA). Three time horizons, within which fluid-bearing channels can exist, were obviously interpreted in terms of main reflectors.

Namely, the 'Top Channel', the 'Base Gas' and the 'Base Canyon'. Using well ties and abridgment of petrophysical knowledge to trace both the fluid contact and coverage, it was a hard kick to pick-up the Base Gas consistently. Whereas picking-up both the Top Gas and Top Channel was relatively consistent and straightforward. Nevertheless, significant uncertainties still exist within the time-converted depth/thickness estimates for such horizons. A total of 4 stratigraphic-control wells, located within the seismic survey coverage, were made available to use for the present seismic forward and inverse modeling trials. Each has a full suite of both sonic and density logs over the target reservoir zone and was petrophysically evaluated in details.

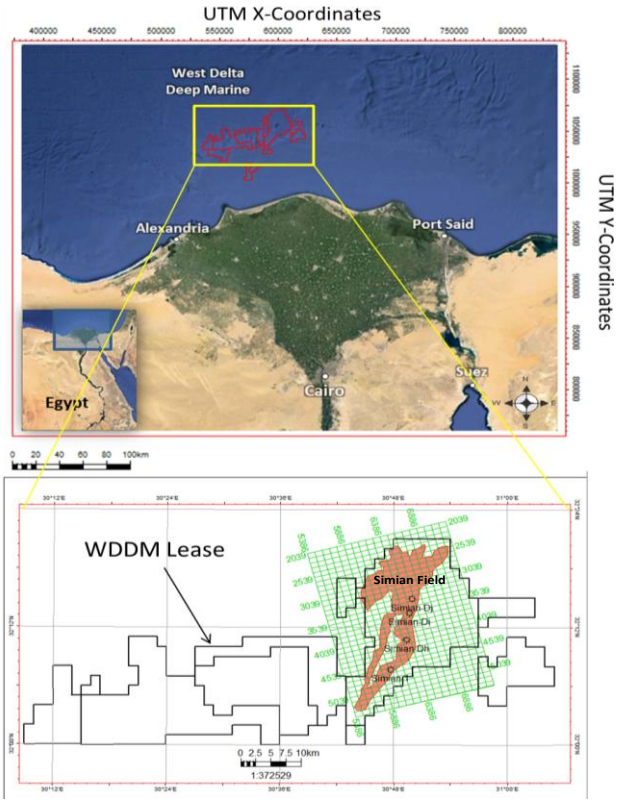

Fig. 1: Satellite image (upper) showing the general location of the Simian gas field within the Egypt's offshore West Delta Deep Marine (WDDM) concession and index map (lower) showing the conducted seismic surveying lines and the available stratigraphic-control wells.

Simian' southern part is made up of both the larger main channel to the east and the smaller central channel to the west, separated by non-reservoir shale-prone intervals. Such separate branches are obviously intervened with highly sinuous, amalgamated, leveed and frontal-splay channel sands. They converge in the north, forming less confined and more bifurcated (labyrinth) sinuous channel sands than in the southern part. Simian' northern/northwestern part is made up of a sheet-like deposit (**Figure 2**).

Post-stack Inversion Theory

Impedance inversion was first discussed and reported in Lindseth [5]. Different approaches have been used for post-stack seismic inversion, including model-based, sparse-spike, band-limited and broad-band among others [6]. In the present study, the robust model-based absolute impedance inversion scheme was mainly used to estimate acoustic impedance volume from the Simian field seismic cube.

Data were forwardly and inversely inverted in 3D using STRATA Seismic Inversion Software (Hampson–Russell Software & Services Limited, USA). In an iterative fashion, a generalized linear approximated solution, over all the contributed seismic traces, is attempting to minimize an objective function J by updating (modifying) the start model parameter(s) (initial guess) until the resulting synthetic seismic traces match the original traces [7] within a certain tolerance level

$$J = weight_1\ x\ (S - W * R) + weight_2\ x\ (M - H * R)$$

Where S is the seismic trace, W is the wavelet, R is the reflectivity which can be extracted from the convolved seismic trace, M is the start model parameter(s) and H is the forward integral (operator) which is convolved with the best-fitted reflectivity to produce the final model at certain iteration. * denotes the convolution process. Data weights are indirectly related to the ambient uncorrelated, random noise with the seismic signal. To assure more realistic results, the linearized solution is usually constrained by well logging/core data or a-prior subsurface geological/geophysical information [8,9].

Inversion Methodology and Results

The initial model was built by vertical blocking (averaging) and lateral interpolating the synthetic acoustic impedances from three stratigraphic-control wells, while the fourth well data was left to verify the overall inversion results and its resolution. The conventionally interpreted three seismic time horizons were introduced in background to guide such a blocking and/or interpolation. Since the quality and reliability of inversion results depends strongly on the wavelet extraction, a careful consistent calibration of seismic to well log data was always maintained within the target reservoir zone. The forwardly-generated synthetic seismic traces, from the convolved earth's wavelet with high-resolution reflectivity (**Figure 3**) within the target reservoir zone, were initially used to update further seismic reflections around and away from each stratigraphic-control well location in multi-sequential (recursive) fashion (**Figure 4**). The start earth model showed a general trend of increasing the impedance but with no significant lateral variations (**Figure 5**). Iteratively, until a satisfied match (root-mean square misfit percentage) was encountered between synthetic (calculated) and original (measured) seismic traces (**Figure 6**), the whole acoustic parameters within the target reservoir zone were then consistently produced.

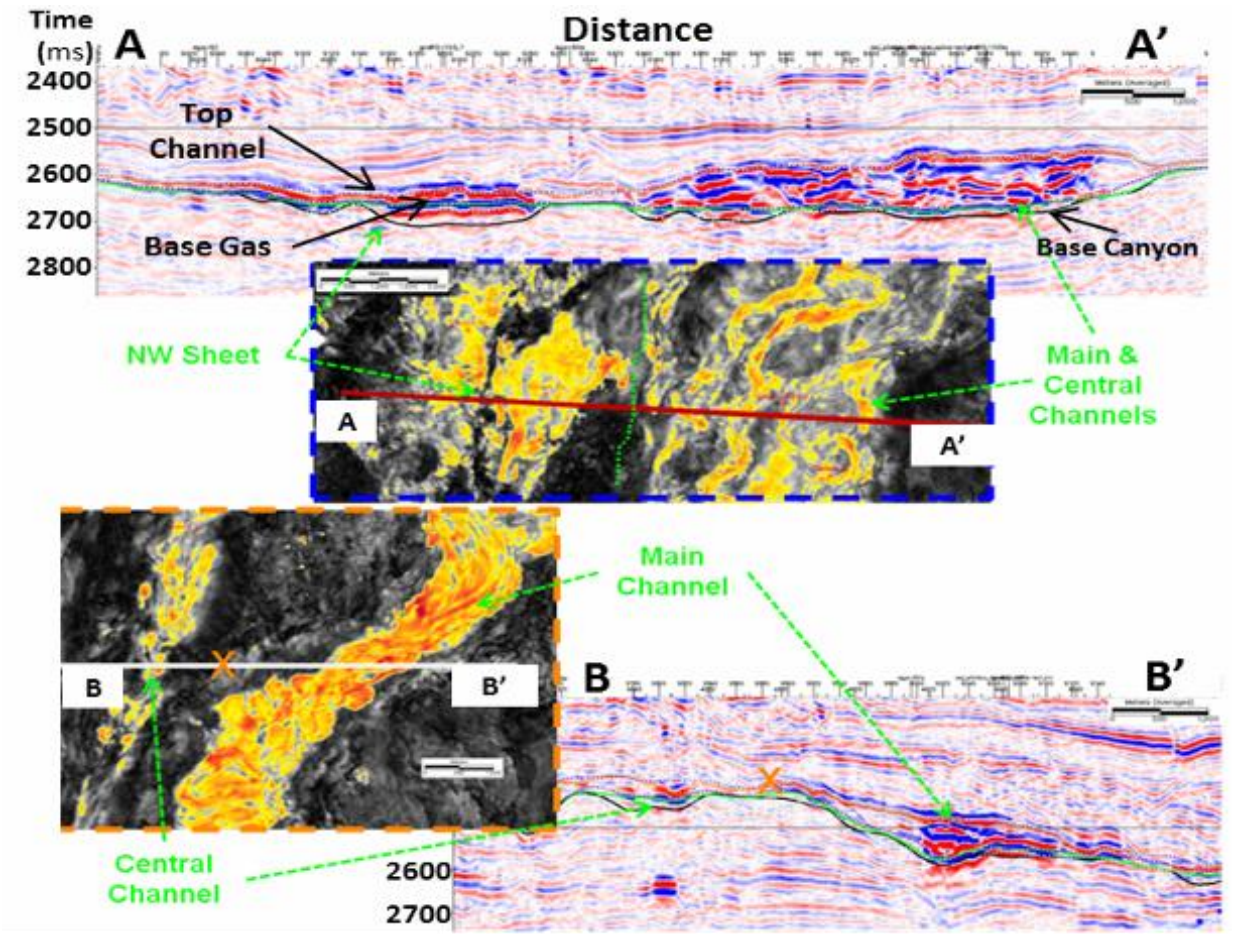

Fig. 2: Typical interpreted two-dimensional (2D) seismic sections and average seismic amplitude (magnitude) slices at the Simian gas field, highlighting the differences in channel architecture of the southern main and central channels (more confined complexes) and the northern/northwestern sheet-like channel (less confined and more bifurcated complexes).

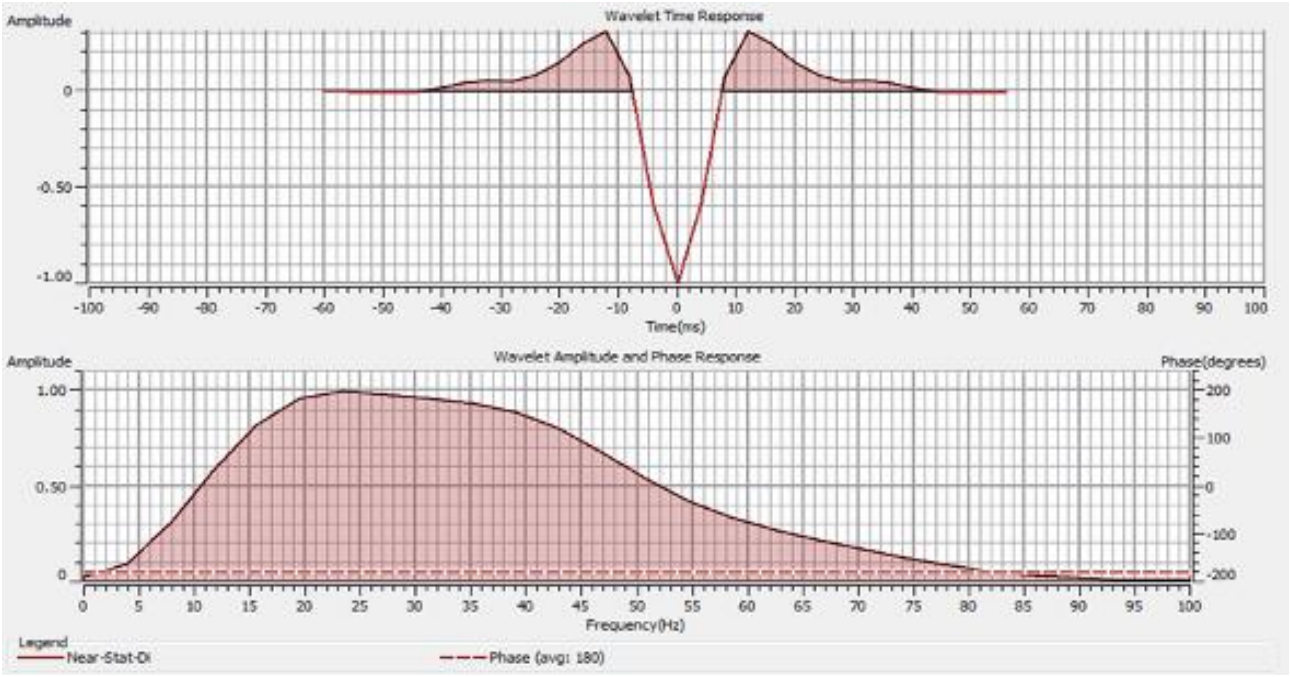

Fig. 3: Estimating both the amplitude and frequency spectra from the extracted optimal wavelets to be used in generating the synthetic seismic traces, upon the convolution with a high-resolution reflectivity series.

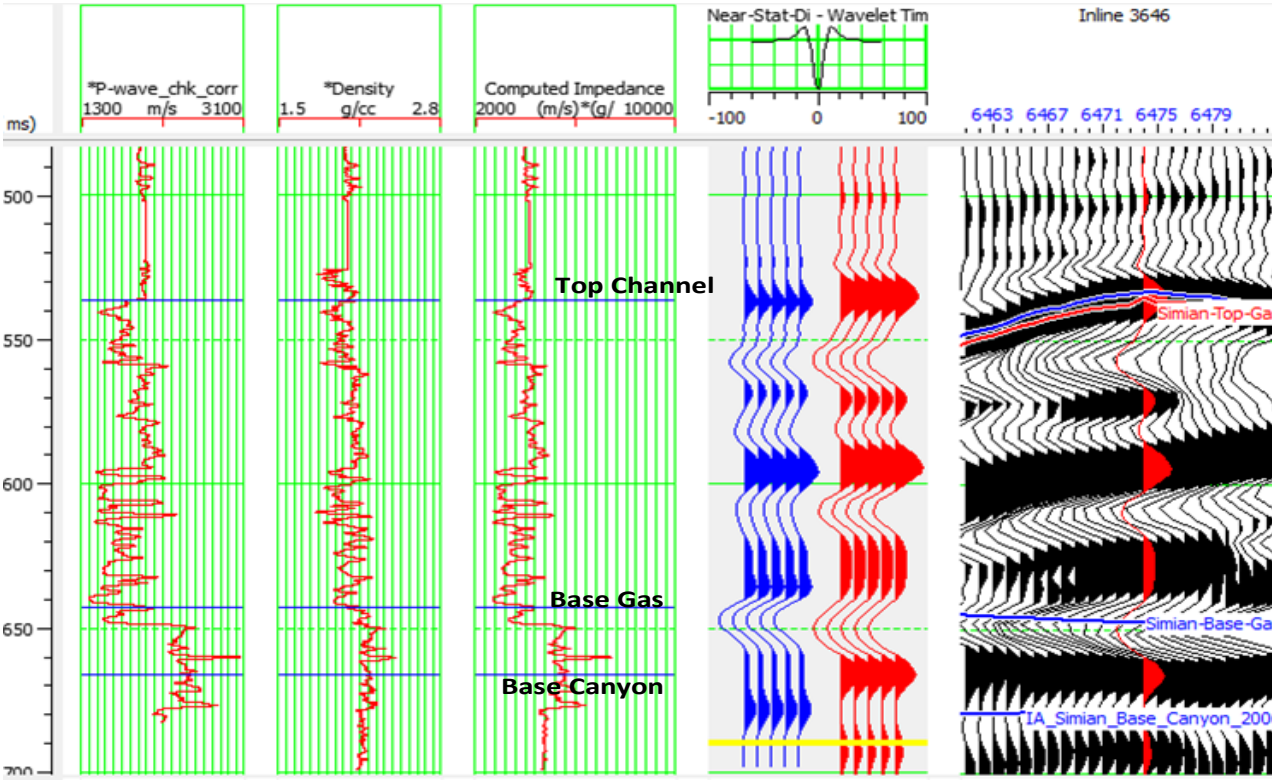

Fig. 4: Typically-generated synthetic seismic traces, from the convolved earth's wavelet with high-resolution reflectivity within the target reservoir zone, which were initially used to update further seismic reflections around the stratigraphic-control well Simian–DJ. Both the synthetic (blue-colored reflections) and original seismic traces (red-colored reflections) are plotted juxtaposed to each other.

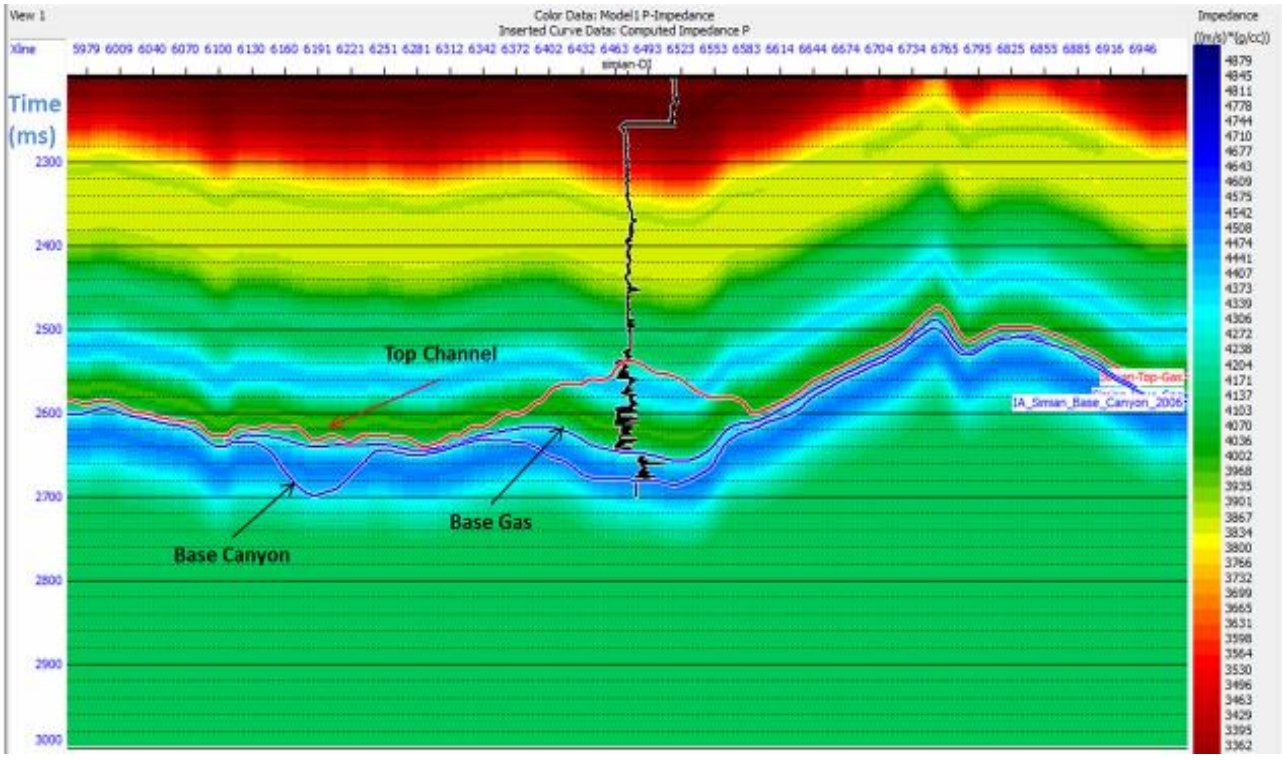

Fig. 5: Typical 2D stitched start earth model (initial guess) which used extensively for updating synthetic seismic traces within the target reservoir zone. The start earth model showed a general trend of increasing the impedance but with no significant lateral variations. Cold colours indicate acoustic impedance highs or more clayey stratigraphic units, while warm colours indicate acoustic impedance lows or more sandy/sandstone stratigraphic units.

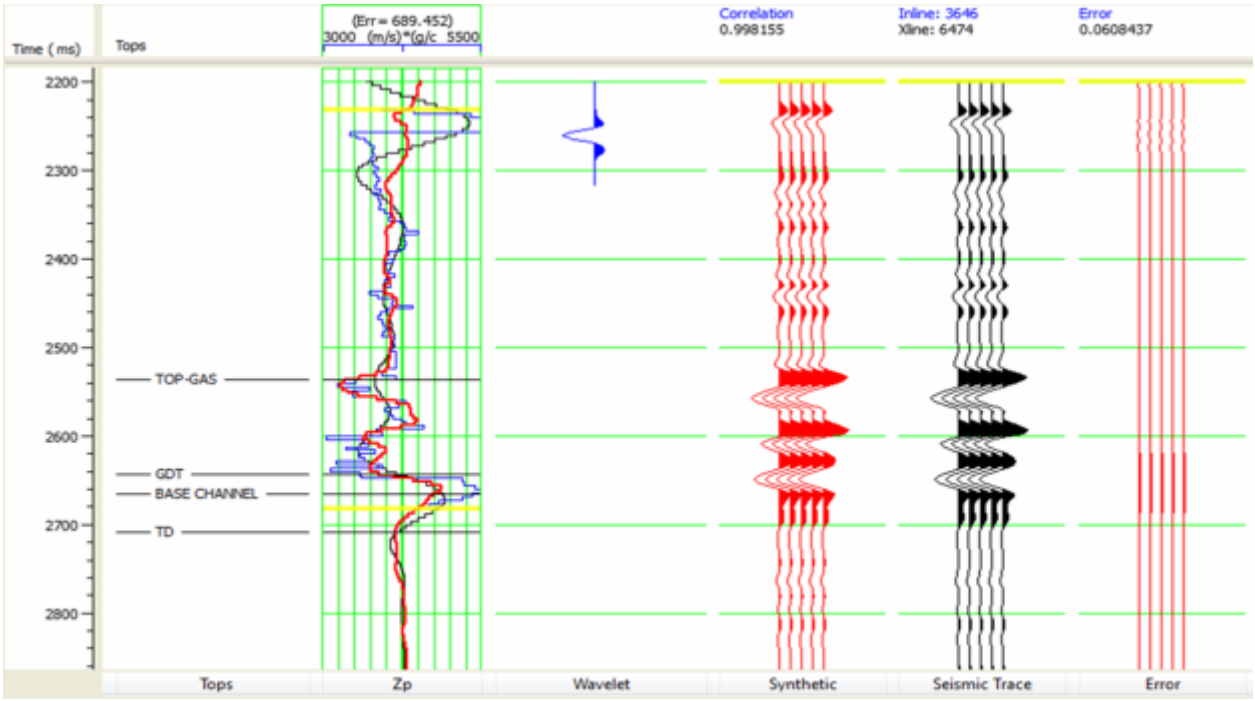

Fig. 6: Typical inversion results analysis at the stratigraphic-control well Simian–DJ where the matching between the synthetic (calculated) and original (measured) seismic traces exceed 99 % within the target reservoir zone. Additionally, the confidence of inversion results was verified by cross-correlation of the resulting inverted acoustic impedance trajectory (red-colored curve) with the original logs data (black-colored curve).

All inversion results were analyzed at the three stratigraphic-control wells, where the matching between the synthetic (calculated) and original (measured) seismic traces exceed 99 % within the target reservoir zone. The confidence of the inversion trials was verified by cross-correlation of the resulting impedance log with the original impedance data at the fourth stratigraphic-control well (**Figure 6**).

Inversion results have highly improved both the vertical and lateral resolutions of the smoothed-earth impedance model than the original seismic reflection volume, quantified the data interpretation flow and could be reasonably used to reduce near-future drilling risk [10]. Inverted impedance volume obviously helped to understand the reservoir architectural style in terms of channel sand geometry, detailed lateral variations and possible fluid coverage within Simian field, where the gas column occupies the lower heterogeneous complexes of it. Correspondingly, the basal sand-rich part of the reservoir will significantly influence aquifer behavior during the production stage. Notably, the general character of the smoothed-earth impedance model still affected by original seismic reflections and indicates that the inversion scheme was dominated by the seismic data (**Figure 7**).

Later on, the results were cross-checked using the simplified coloured relative impedance inversion scheme [11], assuming that the larger the seismic amplitude then the larger the impedance contrast to produce it [12].

In coloured inversion, the zero-phase seismic data are usually rotated by –90^{o} and the seismic data amplitude spectrum is normally reshaped to match the results from impedance logs (**Figure 8**). A satisfied correlation between the encountered smoothed-earth impedance models of both two inversion schemes was obtained, where laterally-extended high acoustic impedance anomaly, representing the gas-bearing sand/sandstone complexes were clearly encountered between time zones 2,650 and 2,700 ms (**Figure 9**).

Concluding Remarks

The present 3D acoustic impedance inversion trials on the stacked–migrated seismic reflection volume at the Simian gas filed were proven to be a useful quantitative technique for the subsurface interpretation, where the channel gas-bearing sand/sandstone geometry, lateral variations and possible fluid coverage of the field were clearly imaged and reliably evaluated. To invert such a high-resolution 3D smoothed-earth impedance model, the initial model parameters have been consistently constrained by the available stratigraphic-control well data, original seismic reflections and a-priori subsurface geological/geophysical information. The confidence of the inversion trials was verified by cross-correlation of the resulting impedance log with the original impedance data at the rest-of-stratigraphic-control well(s).

Acknowledgement

The authors are indebted to both RASHPETCO and the Egyptian General Petroleum Corporation (EGPC) for providing the raw seismic reflection data of the Simian gas field to be used for the present 3D smoothed-earth inversion trials.

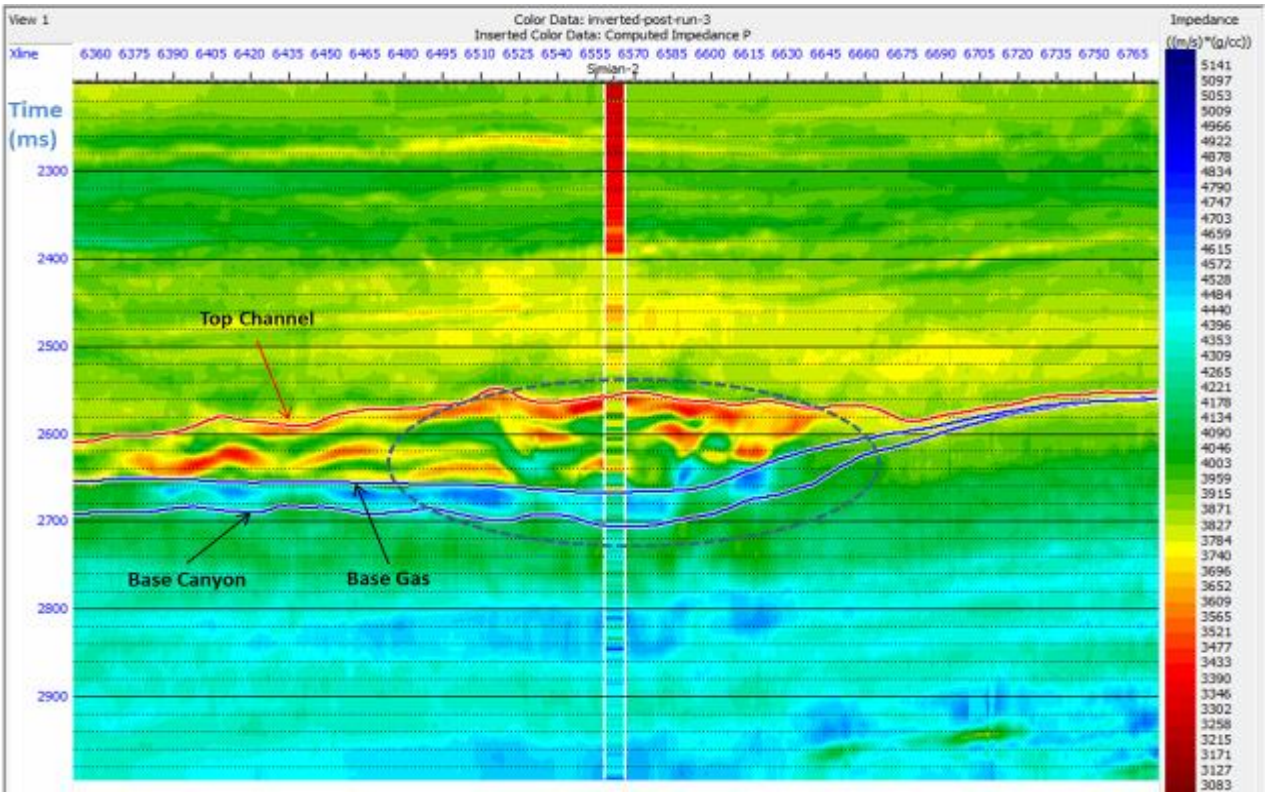

Fig. 7: Typical 2D stitched final inverted earth model, upon using 3D model-based inversion scheme. The laterally-extended high acoustic impedance anomaly was encountered between time zones 2,650 and 2,700 ms. Original (measured) acoustic impedance sounding image is laid over to show a satisfied tie.

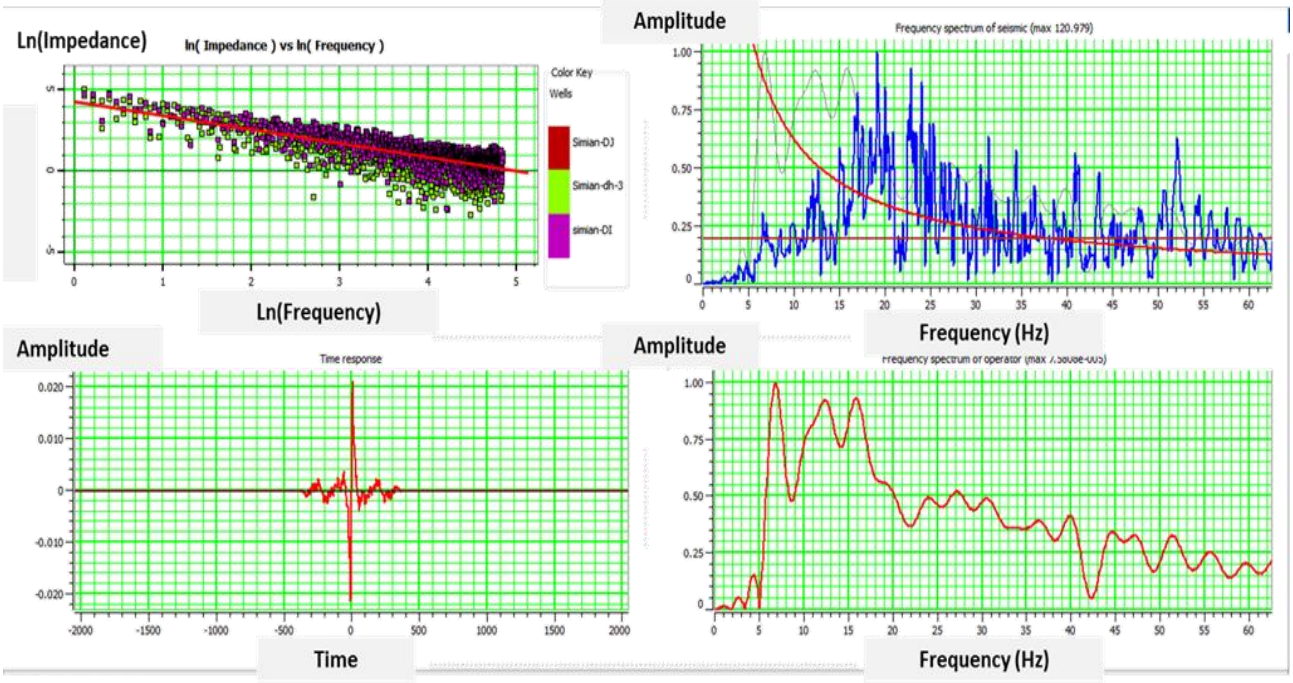

Fig. 8: Operative parameter which is used in the present coloured inversion scheme in both time- (left) and frequency-(right) domains.

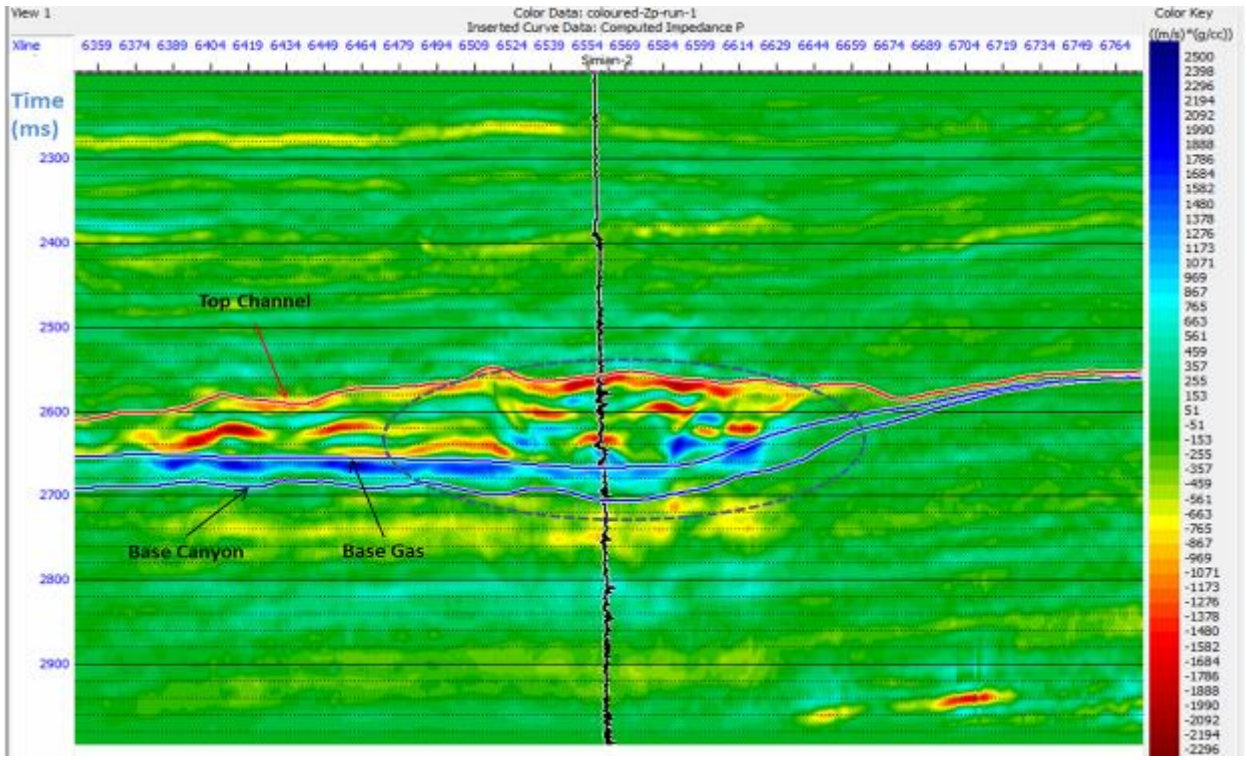

Fig. 9: Typical 2D stitched final inverted earth model, upon using 3D coloured inversion scheme. The laterally-extended high acoustic impedance anomaly was encountered between time zones 2,650 and 2,700 ms. Original (measured) acoustic impedance sounding log is laid over to show a satisfied tie.

References

1) **Tarantola, A. (1987).** Inverse Problem Theory. Elsevier Scientific Publishing Co., Amsterdam.
2) **Cross, N. E., Cunningham, A., Cook, R. J., Taha, A., Esmail E. and El-Swidan N. (2009)**. Three-dimensional seismic geomorphology of a deep-water slope-channel system: The Sequoia field, offshore west Nile Delta, Egypt. AAPG Bulletin, 93, 535–561.
3) **Catterall, V., Redfern, J., Hansen, D. M., Gawthorpe, R., Badalini, G. (2007)**. Controls on the 3D seismic geomorphology of submarine channel systems: Nile Delta slope, Egypt. Petroleum Geosciences Collaboration Conference 2007, 61–62.
4) **Catterall, V., Redfern, J., Gawthorpe, R., Hansen, D. and Thomas M. (2010)**. Architectural Style and Quantification of a Submarine Channel-Levee System Located in a Structurally Complex Area: Offshore Nile Delta. Journal of Sedimentary Research, 80, 991–1017.
5) **Lindseth, R. O. (1979)**. Synthetic sonic logs – A process for stratigraphic interpretation. Geophysics, 44, 3–26.
6) **Russell, B. and Hampson, D. (1991)**. Comparison of post-stack inversion methods. 61st SEG Annual International Meeting (Expanded Abstracts), 10, 876–878.
7) **Cooke, D. A. and Schneider, W. A. (1983)**. Generalized linear inversion of reflection seismic data. Geophysics, 48(6), 665–676.
8) **Tonn, R. (1998)**. Seismic reservoir characterization of Montney sand in the Peace River Arch area, Canada. The Leading Edge, 17, 643–646.
9) **Hill, S. J. (2005)**. Inversion-based thickness determination. The Leading Edge, 24(5), 477–480.
10) **Pendrel, J. (2006).** Seismic Inversion – A Critical Tool in Reservoir Characterization. Scandinavian Oil–Gas Magazine, 5/6, 19–22.
11) **Lancaster, S. and Whitcombe, D. (2000).** Fast-track Coloured Inversion. 70th SEG Annual International Meeting (Expanded Abstracts), 19, 1572–1575.
12) **Hicks, G. (2008)**. Seismic Inversion: Which Why Where When? Basin and Reservoir. The Newsletter for BG Group Geoscientists and Engineers, 37, 18–24.